Ozone Comparison between Pandora #34, Dobson #061, OMI, and OMPS at Boulder Colorado for the period December 2013 – December 2016.

Jay. Herman[1], Robert Evans[4], Alexander Cede[3], Nader Abuhassan[1], Irina. Petropavlovskikh[2], Glenn McConville[2], Koji Miyagawa[5], and Brandon Noirot[2]

[1] University of Maryland Baltimore County (JCET) at Goddard Space Flight Center, Greenbelt, MD
[2] NOAA Earth System Research Laboratory, Boulder, CO. Cooperative Institute for Research in Environmental Sciences (CIRES), University of Colorado, Boulder, CO
[3] LuftBlick, Austria and Goddard Space Flight Center, Greenbelt, MD
[4]Former scientist at NOAA/ESRL/GMD, Boulder, CO: Retired
[5]Guest Scientist at NOAA/ESRL/GMD, Boulder, CO

Abstract

A one-time calibrated (in December 2013) Pandora Spectrometer Instrument (Pan #034) has been compared to a periodically calibrated Dobson spectroradiometer (Dobson #061) co-located in Boulder, Colorado, and compared with two satellite instruments over a 3-year period (December 2013 – December 2016). The results show good agreement between Pan#034 and Dobson#061 within their statistical uncertainties. Both records are corrected for ozone retrieval sensitivity to stratospheric temperature variability obtained from the Global Modeling Initiative (GMI) and Modern-Era Retrospective analysis for Research and Applications (MERRA-2) model calculations. Pandora#034 and Dobson#061 differ by an average of 2.1 ± 3.2 % when both instruments use their standard ozone absorption cross sections in the retrievals algorithms. The results show a relative drift (0.2 ± 0.08% per year) between Pandora observations against NOAA Dobson in Boulder, CO over a three-year period of continuous operation. Pandora drifts relative to the satellite Ozone Monitoring Instrument OMI and the Ozone Mapping Profiler OMPS are +0.18 ± 0.2 % per year and -0.18 ± 0.2 % per year, respectively, where the uncertainties are two standard deviations. The drift between Dobson #061 and OMPS for a 5.5-year period (January 2012 – June 2017) is -0.07 ± 0.06 % per year.

Author(s): Jay Herman et al.
MS No.: amt-2017-157
MS Type: Research article
Iteration: Revised
Special Issue: Quadrennial Ozone Symposium 2016 Status and trends of atmospheric ozone (ACP/AMT inter-journal SI)

Introduction

A Pandora Spectrometer Instrument #034 (PSI) located on top of the NOAA building in Boulder, Colorado has been operating since December 2013 with little maintenance and using the original calibration. The purpose of this paper is to present a comparison between two co-located ozone measuring instruments, Pandora #034 and Dobson #061 for the period December 2013 to December 2016. Additional comparisons are made with satellite overpass data from OMI (Ozone Monitoring Instrument on board the AURA spacecraft) and OMPS (Ozone Mapping Profiler Suite on board the Suomi NPOESS satellite). This paper is an extension of a previously published paper (Herman et al., 2015) that presented just 1 year of data. The results demonstrate the accuracy and stability of both the Dobson and PSI for retrieval of total column ozone, and serves as a validation demonstration at one location for both the fairly new PSI and for satellite ozone data from OMI and OMPS. Part of the experiment comparing Pandora #034 to Dobson #061 was to see if Pandora #034 would perform well over a long period without additional calibration or adjustments. The only change made during the period 2014 to the present (August 2017) was to replace a broken motor on the suntracker that caused a data gap in early 2016.

The characteristics of both the PSI and the Dobson Spectroradiometer are described in Herman et al. (2015). Briefly, the PSI consists of a small Avantes low stray light spectrometer (280 – 525 nm with 0.6 nm spectral resolution with 5 times oversampling) connected to an optical head by a 400 micron core diameter single strand fiber optic cable. The spectrometer is temperature stabilized at $20^{O}C$ inside of a weather resistant container. The optical head consists of a collimator and lens giving rise to a 2.5^{O} FOV (field of view) FWHM (Full Width Half Maximum) with light passing through two filter wheels containing diffusers, open hole, a UV340 filter (blocks visible light), neutral density filters, and an opaque position (dark current measurement). The optical head is connected to a small suntracker capable of accurately following the sun's center using a small computer-data logger contained in a weatherproof box along with the spectrometer. Pandora#034 is capable of obtaining NO_2 and Total Column Ozone TCO amounts sequentially over a period of 80 seconds. The integration time in bright sun is about 4 milli-seconds that is repeated and averaged for 30 seconds to obtain very high signal to noise and an ozone precision of less than 1 DU or 0.2% (1 DU = 2.69×10^{16} molecules/cm^{2}).

The Dobson record in Boulder started in 1966 based on an improved design from the instrument first deployed in the 1920's (Dobson, 1931). Dobson instrument uses a differential absorption method to derive total column ozone from direct–sun measurements using two UV wavelength pairs in the 300 – 340 nm range (see Herman et al., 2015). The extensive Dobson network uses the Bass-Paur (BP) ozone absorption cross sections (Bass and Paur, 1985) for operational data processing (Komhyr et al., 1993).

All NOAA Dobson instruments are periodically calibrated against WMO world standard Dobson #083, which in turn uses Langley method calibrations at the Mauna Loa Observatory station (Komhyr et al., 1989). Standard lamps are used to check Dobson spectral registration stability. Recently, July 2017, intermediate calibrations from Dobson #083 were applied to the Dobson #061 ozone data record that improved its comparison with satellite data (the calibration updates were processed by one of the co-authors, Koji Miyagawa).

The main sources of noise in the PSI measurement comes from the presence of clouds or haze in the FOV, which increases the exposure time needed to fill the CCD wells to 80% and reduces the number of measurements in 30 seconds. For this comparison study, data were selected for scenes that are clear-sky conditions as determined from the Dobson A-D pair direct-sun data record.

Accuracy in the PSI spectral fitting retrieval is obtained using careful measurements of the spectrometer's slit function, wavelength calibration, and knowledge of the solar spectrum at the top of the atmosphere. The current operational PSI ozone retrieval algorithm used in this study is based on extraterrestrial solar flux from a combination of the Kurucz spectrum (wavelength resolution $\lambda/1\lambda = 500\ 000$) radiometrically normalized to the lower-resolution shuttle Atlas-3 SUSIM spectrum (Van Hoosier, 1996; Bernhard et al., 2004, 2005), BDM ozone cross sections (Brion et al. (1993, 1998) and Malicet et al. (1995)), corrections for stray light, and an effective ozone weighted temperature.

The Dobson data used in this study contain the individual measurements (more than 1 per day between 09:00 and 15:00 local time with almost all of the data between 10:00 and 14:00) for clear-sky direct-sun observations using the quartz plate and A-D wavelength pairs for ozone retrieval (Dobson label ADDSGQP). These were made available by one of the co-authors (I. Petropavlovskikh, private communication, Table 2). The NOAA Dobson total ozone data are typically archived at WOUDC (World Ozone and Ultraviolet Radiation Data Centre) or NDACC (Network for the Detection of Atmospheric Composition Change) with one representative ozone value per day.

1. Temperature Sensitivity

The PSI ozone retrieval algorithm is more sensitive to the effective ozone weighted average temperature than is the 4 wavelength Dobson retrieval (Redondas et al., 2014). Neglecting the temperature sensitivity creates a seasonal difference between the two instruments. To correct for this, we use an effective ozone temperature T_E based on daily ozone profile weighted altitude temperature averages (Redondas et al., 2014). The temperature and ozone profile data were obtained from the GMI (Global Modeling Initiative) model calculation for 2012 to 2016. (https://gmi.gsfc.nasa.gov/merra2hindcast/). The GMI model provides atmospheric composition hindcasts using MERRA-2 (Modern-Era Retrospective analysis for Research and Applications, Version 2, meteorology (Strahan et al., 2013; Wargan and Coy, 2012) https://gmao.gsfc.nasa.gov/reanalysis/MERRA-2/). The simulation with 2 x 2.5 degree resolution uses the CCMI (Chemistry–Climate Modelling Initiative, Morgenstern et al., 2017) emissions and boundary conditions. MERRA-2 uses assimilation schemes based on hyperspectral radiation, microwave observations and ozone satellite measurements. The resulting seasonal cycle for T_E shows variations over the four year period, while day-to-day variability is enhanced during winter and spring season (Fig. 1). An estimated 5th year (2017) has been added (Fig. 1) by forming the average of the daily temperatures from the 2013 to 2016 period.

The T_E time series data are used for an ozone retrieval temperature correction TCO_{cor} coefficient per ^{O}K given in the form $TCO_{corr} = TCO\ (1 + C(T))$ and $O_3(corr) = O_3\ TCO_{corr}$ (Herman et al., 2015), where $C(T_E)$ is given by eqns. 1 and 2.

$$C_{Pandora\text{-}BDM}(T_E) = 0.00333(T_E - 225) \qquad \text{(Herman et al., 2015)} \qquad (1)$$

$$C_{Dobson\text{-}BP}(T_E) = -0.0013(T_E - 226.7) \qquad \text{(Redondas et al., 2014)} \qquad (2)$$

$$C_{Dobson\text{-}BDM}(T_E) = 0.00042(T_E - 226.7) \qquad \text{(Redondas et al., 2014)} \qquad (3)$$

As mentioned earlier, the Dobson TCO retrieval normally uses the Bass and Paur (BP) ozone absorption coefficients, while Pandora uses the Brion-Daumont-Malicet (BDM) coefficients. A change in T_E of $+1^{O}$ change leads to TCO changes for the Pandora(BDM), Dobson(BP), and Dobson(BDM) instruments of +0.33%, -0.13%, and 0.042%, respectively. For a nominal TCO value of 325 DU, the change would be +1.1 and -0.4 DU, a net relative change of 1.5 DU for a $1^{O}K$ change between Pandora(BDM) and Dobson(BP).

While BDM cross sections are not currently recommended for use in standard Dobson processing, their use yields slightly different values of TCO and a smaller sensitivity to temperature. The basic Dobson algorithm, based on pairs of wavelengths, is intrinsically less sensitive to T_E than Pandora's spectral fitting retrieval.

2. TCO Comparisons between Pandora, Dobson, OMI and OMPS

Comparing retrieved TCO from the PSI, Dobson, OMI and OMPS instruments show that there are small, but significant differences between the PSI and Dobson instruments and between the ground-based instruments and satellite derived values of TCO. The difference is calculated using three-year estimates of secular change based on a linear least squares fit to the percent differences between the instruments. The cloud-free direct-sun A-D pair Dobson ozone data are selected for comparison with time-matched Pandora#034 retrieved ozone data (Herman et al., 2015). The Pandora#034 retrieved ozone (every 80 seconds) are matched to the less frequent

Dobson#061 retrieval times that are obtained for mid-day solar zenith angles (SZAs) and averaged over ±8 minutes (Fig. 2A).

Each clear-sky PSI data point is an average of 2000 (early morning to evening SZAs) to 4000 (mid-day SZAs) measurements obtained during 30 seconds. All data for this study were clear-sky within the instrument's field of view based on the Dobson criteria for A-D-pair direct-sun clear sky. In addition, the PSI data are averaged over a period of +/- 8 minutes surrounding the Dobson time of measurement (2 to 3 times per day). Since PSI measurements are obtained every 80 seconds, there were an additional 10 PSI data points averaged together to compare to each Dobson, OMI, or OMPS measurement. The result is high signal to noise values for Pandora and high precision (0.1%). The same procedure using cloud-screened PSI data was used for comparisons with OMI and OMPS, where they measure once or twice per day over Boulder, Colorado. Some of the variations in the day to day ozone values are driven by changes in the local weather over Boulder, Colorado (see Fig. 14 in Herman et al., 2015), with weekly averages having much smaller variation.

Figure 2B shows a Lowess(0.1) fits to the two time series in Fig. 2A that is approximately equivalent to a 3-month running average. The Lowess(f) procedure is based on local least squares fitting using low order polynomials applied to a specified fraction f of the data (Cleveland, 1979) that reduces the effect of outlier points from the mean. The smooth curves show a small variable difference between the Dobson and Pandora time series. Fig. 2C shows the percent difference PD between the time series in Fig. 2A and the residual seasonal variation in PD. Estimating the slope of the least squares fit to the percent difference can be sensitive to the selection of the end points of the time series. This effect can be minimized by removing the seasonal time dependence (Fig. 2C) using a low-pass filter function with zero slope derived from the Lowess(0.1) fit. The result is shown in Fig. 3A.

Figure 3 shows the de-seasonalized percent differences PD(A,B) for six pairs between Pandora #034, Dobson #061, OMI, and OMPS for the 3-year period 2014 – 2016 (summarized in Table 1). The slightly curvy Lowess (0.1) lines about each linear fit show the residual seasonal cycles, which are too small to have an effect on slope determination. Error estimates (Fig. 3 and Table 1) for the linear least squares slopes and averages are one standard deviation (1-STD). Some of the error estimates are large enough to make the statistical significance of the slopes marginal (see Panel E OMPS vs Pandora; 0.18 ± 0.098, $p = 0.06$), while others are significant (see Panel D OMI vs Dobson: -0.18 ± 0.08, $p = 0.03$) at the 2-STD level. The significance probability parameter p is given, where p is the probability (0 to 1) that the slope is statistically different from 0 relative to $p = 0.05$. Also shown are the numbers of data points in each time series.

After removal of the residual seasonal variation in the calculated percent differences, there still is a statistically significant drift of 0.2% per year ($p < 0.001$) between the Pandora#034 and Dobson#061 (Panels A and B in Fig. 3) using either BP or BDM ozone cross sections for Dobson#061. The differences in the mean values (-2.1 and -2.8%) are not significant at the 2-STD level.

The linear trend (Panel C, -0.09 ± 0.08 % per year, p = 0.3) between the Dobson and OMPS is not significantly different from zero, while the drift with OMI (Panel D,-0.18 ± 0.08 % per year, p = 0.03) is significant. This suggests that OMI ozone retrievals are drifting with respect to OMPS and the Dobson. Extending the period from 2012 to June 2017 gives a very small, but significant trend, -0.07 ± 0.03 % per year, p = 0.047 for PD(OMPS,Dobson).

Calculations for Pandora#034 (Panels E and F in Fig. 3) show marginally significant (p = 0.06) trends for Pandora#034 compared to OMPS (Panel E, -0.18 ± 0.098 % per year) and OMI (Panel F, +0.18 ± 0.096 % per year). If the Pandora#034 time series is extended into 2017 to minimize the effect of missing Pandora data in 2016, then the trends for Pandora compared to OMPS (-0.2 ± 0.08 % / Year p = 0.013) and OMI (0.15 ± 0.076 p=0.05) are significant, but not different from the shorter 2014 – 2016 period. The secular trends for the difference between Pandora#034 and Dobson#061 (-0.2% per year) are almost the same for both Dobson BP and BDM ozone absorption coefficients even though the temperature sensitivity using the Dobson BDM ozone absorption coefficients is small (0.042% per ^{O}C). This suggests that the stratospheric effective ozone temperature change is not a source for the small differences between Pandora#034 and Dobson#061.

Figure 4 shows that the TCO between Pandora#034 and Dobson#061 are highly correlated with 1:1 slope and the correlation coefficient $r^2 = 0.97$ for the 3-year period 2014 to 2016. Similar correlation plots (Fig. 5) for Pandora#034 and Dobson#061 with OMI and OMPS also show very high correlations. The correlations in TCO are obtained after only temperature corrections to Pandora#034 and Dobson#061 using T_E (TCO pairs similar to Fig. 2, panel A).

The Pandora, OMI, and OMPS data used in this study are from the overpass files located on the public websites (Table 2).

Summary

Temperature corrected Pandora#034 and Dobson#061 differ by an average of 2.1 ± 3.2 % with Pandora using its standard retrieval BDM ozone absorption cross sections and Dobson using the recommended BP ozone absorption cross sections. Pandora compared to Dobson shows a small, but significant drift (-0.2 ± 0.08 % per year, $p < 0.001$) for the 2014 – 2016 period. Comparisons of Pandora with OMI and OMPS are marginally significant drifts of 0.18±0.2 and -0.18±0.2 p=0.06 for 2014-2016, but are significant (0.15 ± 0.15 % per year, p=0.05 and -0.2 ± 0.16 % per year, p = 0.013, respectively), if the period is extended to mid-

2017 to minimize the effect of missing Pandora data during 2016. The small Pandora and Dobson trends compared to OMPS suggest that both instruments are stable. The conclusion is that the periodically calibrated Dobson#061 is able to detect smaller ozone trends than a Pandora instrument with no intermediate calibration during a 3-year period. The longer term trend for Dobson compared to OMPS for a 5.5-year period (2012 – June 2017) is -0.07 ± 0.06 % per year, p = 0.047. All error estimates are two STD.

Acknowledgement: The authors would like to thank Dr. Susan Strahan and the MERRA-2 team for supplying the atmospheric temperature data for Boulder, Colorado.

References

Bass, A. M. and Paur, R. J.: The ultraviolet cross-sections of ozone, I, The measurements, in: Atmospheric Ozone, edited by: Zerefos, C. S., Ghazi, A., and Reidel, D., Norwell, Mass., 606–610, 1985.

Bernhard, G., Booth, C. R., and Ehramjian, J. C.: Version 2 data of the National Science Foundation's Ultraviolet Radiation Monitoring Network: South Pole, J. Geophys. Res., 109, D21207, doi:10.1029/2004JD004937, 2004.

Bernhard, G., Evans, R. D., Labow, G. J., and Oltmans, S. J.: Bias in Dobson total ozone measurements at high latitudes due to approximations in calculations of ozone absorption coefficients and air mass, J. Geophys. Res, 110, D10305, doi:10.1029/2004JD005559, 2005.

Brion, J., Chakir, A., Daumont, D., Malicet, J., and Parisse, C.: High-resolution laboratory absorption cross section of O3 Temperature effect, Chem. Phys. Lett., 213, 610–612, 1993.

Brion, J., Chakir, A., Charbonnier, J., Daumont, D., Parisse, C., and Malicet, J.: Absorption spectra measurements for the ozone molecule in the 350–830 nm region, J. Atmos. Chem., 30, 291–299, 1998.

Cleveland, William S., Robust Locally Weighted Regression and Smoothing Scatterplots, Journal of the American Statistical Association, Vol. 74, No. 368. , pp. 829-836, 1979.

Dobson, G. M. B. (1931), A photoelectric spectrophotometer for measuring the amount of atmospheric ozone, Proc. Phys. Soc., 43, 324–339, 1931.

Herman, J.R**.,** R.D. Evans, A. Cede, N.K. Abuhassan, I. Petropavlovskikh, and G. McConville, Comparison of Ozone Retrievals from the Pandora Spectrometer System and Dobson Spectrophotometer in Boulder Colorado, Atmos. Meas. Tech., 8, 3407–3418, 2015, doi:10.5194/amt-8-3407-2015.

Komhyr, W. D., R. D. Grass, and R. K. Leonard (1989), Dobson spectrophotometer 83: A standard for total ozone measurements, 1962–1987, J. Geophys. Res., 94(D7), 9847–9861, doi:10.1029/JD094iD07p09847, 1989.

Komhyr, W. D., C. L. Mateer, and R. D. Hudson (1993), Effective Bass-Paur 1985 ozone absorption coefficients for use with Dobson ozone spectrophotometers, J. Geophys. Res., 98(D11), 20451–20465, doi:10.1029/93JD00602, 1993.

Malicet, J., Daumont, D., Charbonnier, J., Parisse, C., Chakir, A., and Brion, J.: Ozone UV spectroscopy. II. Absorption cross sections and temperature dependence, J. Atmos. Chem., 21, 263–273, 1995.

Morgenstern, Olaf, Michaela I. Hegglin, Eugene Rozanov, Fiona M. O'Connor, N. Luke Abraham, Hideharu Akiyoshi, Alexander T. Archibald, Slimane Bekki, Neal Butchart, Martyn P. Chipperfield, Makoto Deushi, Sandip S. Dhomse, Rolando R. Garcia, Steven C. Hardiman, Larry W. Horowitz, Patrick Jöckel, Beatrice Josse, Douglas Kinnison, Meiyun Lin, Eva Mancini, Michael E. Manyin, Marion Marchand, Virginie Marécal, Martine Michou, Luke D. Oman, Giovanni Pitari, David A. Plummer, Laura E. Revell, David Saint-Martin, Robyn Schofield, Andrea Stenke, Kane Stone, Kengo Sudo, Taichu Y. Tanaka, Simone Tilmes, Yousuke Yamashita, Kohei Yoshida, and Guang Zeng, Review of the global models used within phase 1 of the Chemistry–Climate Model Initiative (CCMI), Geosci. Model Dev., 10, 639-671, https://doi.org/10.5194/gmd-10-639-2017, 2017.

Redondas, A., Evans, R., Stuebi, R., Köhler, U., and Weber, M.: Evaluation of the use of five laboratory-determined ozone absorption cross sections in Brewer and Dobson retrieval algorithms, Atmos. Chem. Phys., 14, 1635–1648, doi:10.5194/acp-14-1635-2014, 2014

Strahan, S.E., A.R. Douglass, and P.A. Newman (2013), The contributions of chemistry and transport to low Arctic ozone in March 2011 derived from Aura MLS Observations, J. Geophys. Res., 118, doi:10.1002/jgrd.50181, 2013.

Van Hoosier, M. E.: Solar ultraviolet spectral irradiance data with increased wavelength and irradiance accuracy, SPIE Proceedings, 2831, 57–64, 1996.

Wargan, K. and L. Coy, 2016: Strengthening of the Tropopause Inversion Layer during the 2009 Sudden Stratospheric Warming: A MERRA-2 Study. Journal of the Atmospheric Sciences, 73, 1871–1887, doi: 10.1175/JAS-D-15-0333.1, 2016.

Tables

Table 1 Percent Difference Summary of Linear Fit Slopes and Mean Differences in Fig. 3

Percent Diff(A,B)	Slope (% per Year)	Probability	Mean (%)	Points	Panel
Pan, Dob(BP)	-0.2 ± 0.04	P < 0.001	-2.1 ± 1.6	2020	A
Pan, Dob(BDM)	-0.2 ± 0.04	P < 0.001	-2.8 ± 1.6	2020	B
OMPS, Dob(BP)	-0.09 ± 0.08	P = 0.3	-1.4 ± 2.1	854	C
OMI, Dob(BP)	-0.18 ± 0.08	P = 0.03	-1.4 ± 1.9	654	D
OMPS, Pan	-0.18 ± 0.098	P = 0.06	0.96 ± 2.7	952	E
OMI, Pan	+0.18 ± 0.096	P = 0.06	1.1 ± 2.1	624	F

Table 2 Data Availability

OMI:
https://avdc.gsfc.nasa.gov/index.php?site=1593048672&id=28/aura_omi_l2ovp_omto3_v8.5_boulder.co_067.txt
OMPS:
ftp://toms.gsfc.nasa.gov/pub/omps_tc/overpass/suomi_npp_omps_l2ovp_nmto3_v02_boulder.co_067.txt
Pandora34:
https://avdc.gsfc.nasa.gov/pub/DSCOVR/Pandora/DATA/Boulder/Pandora34/L3c/
Dobson061:
ftp://aftp.cmdl.noaa.gov/data/ozwv/Dobson/WinDobson/Pandora%20comparisons/Dobson61%20Boulder%20Ad-dsgqp%20120213-032717_w_Header.txt

Figure Captions

Fig. 1 Calculated T_E using model estimates of O_3 and temperature profiles. The Trend is calculated from the difference of T_E from its 4-year daily mean that is also used for year 2017 labelled Avg.

Fig. 2 Panel A shows the retrieved ozone time series (December 2013 – June 2017) for Pandora (red) and Dobson (Black). Panel B shows Lowess(0.1) fit to the each time series. Panel C shows the percent difference, a linear least squares fit, and a Lowess(0.1) fit showing seasonal residuals.

Fig. 3 Comparisons of Pandora(BDM) with Dobson(BP and BDM) retrieved ozone for Boulder, Colorado in percent differences of retrieved ozone and comparisons with OMI and OMPS. Slope = value of the linear least square fit, ±N is 1 STD, and p is the probability (0 to 1) that the slope is statistically different from 0 relative to $p = 0.05$. The solid lines are a Lowess(0.1) fit and a linear least squares fit.

Fig. 4 Correlation between Pandora #034 and Dobson #061: 2014 – 2016

Fig. 5 Correlation of Pandora#034 and Dobson#061 with OMI and OMPS: 2014 - 2016

Figures

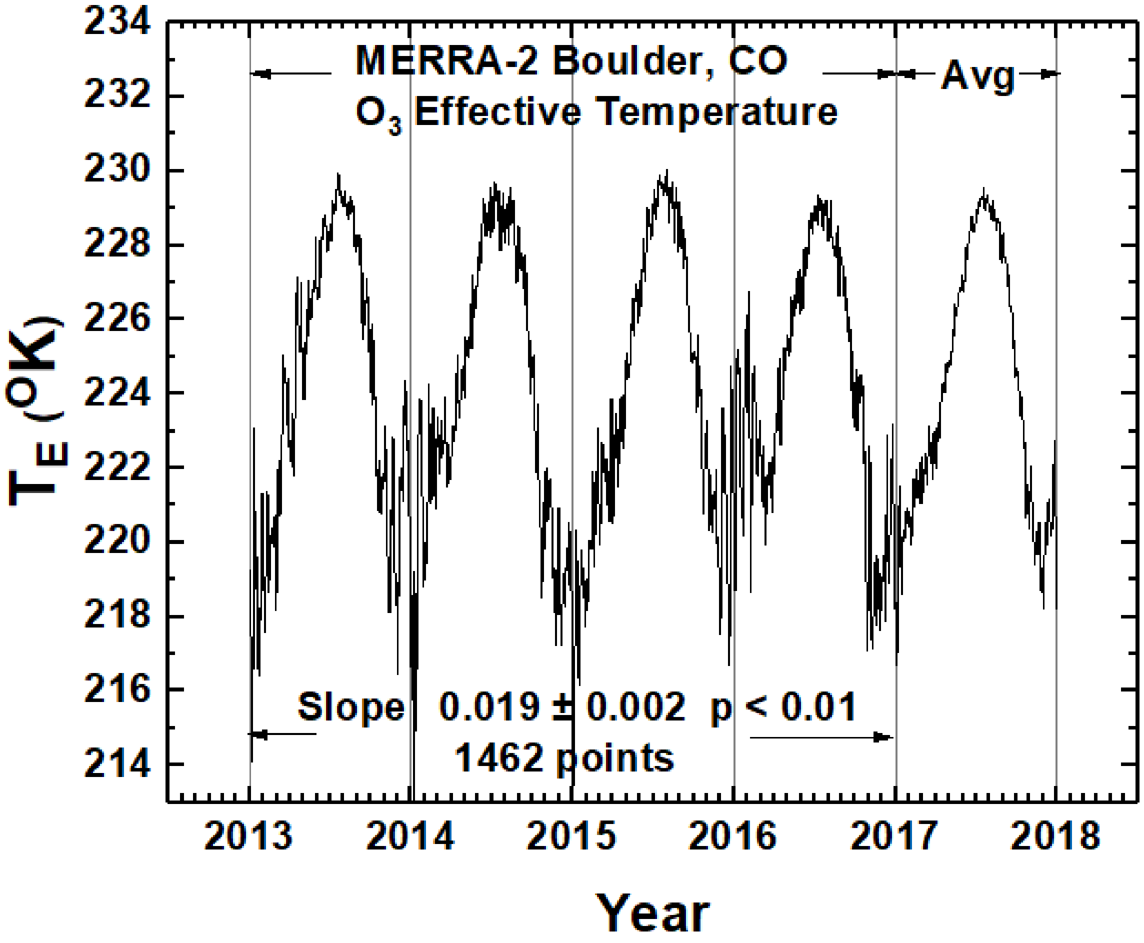
MERRA-2 Boulder, CO
O$_3$ Effective Temperature
Avg
Slope 0.019 ± 0.002 p < 0.01
1462 points
T$_E$ (°K)
234
232
230
228
226
224
222
220
218
216
214
2013
2014
2015
2016
2017
2018
Year

F1

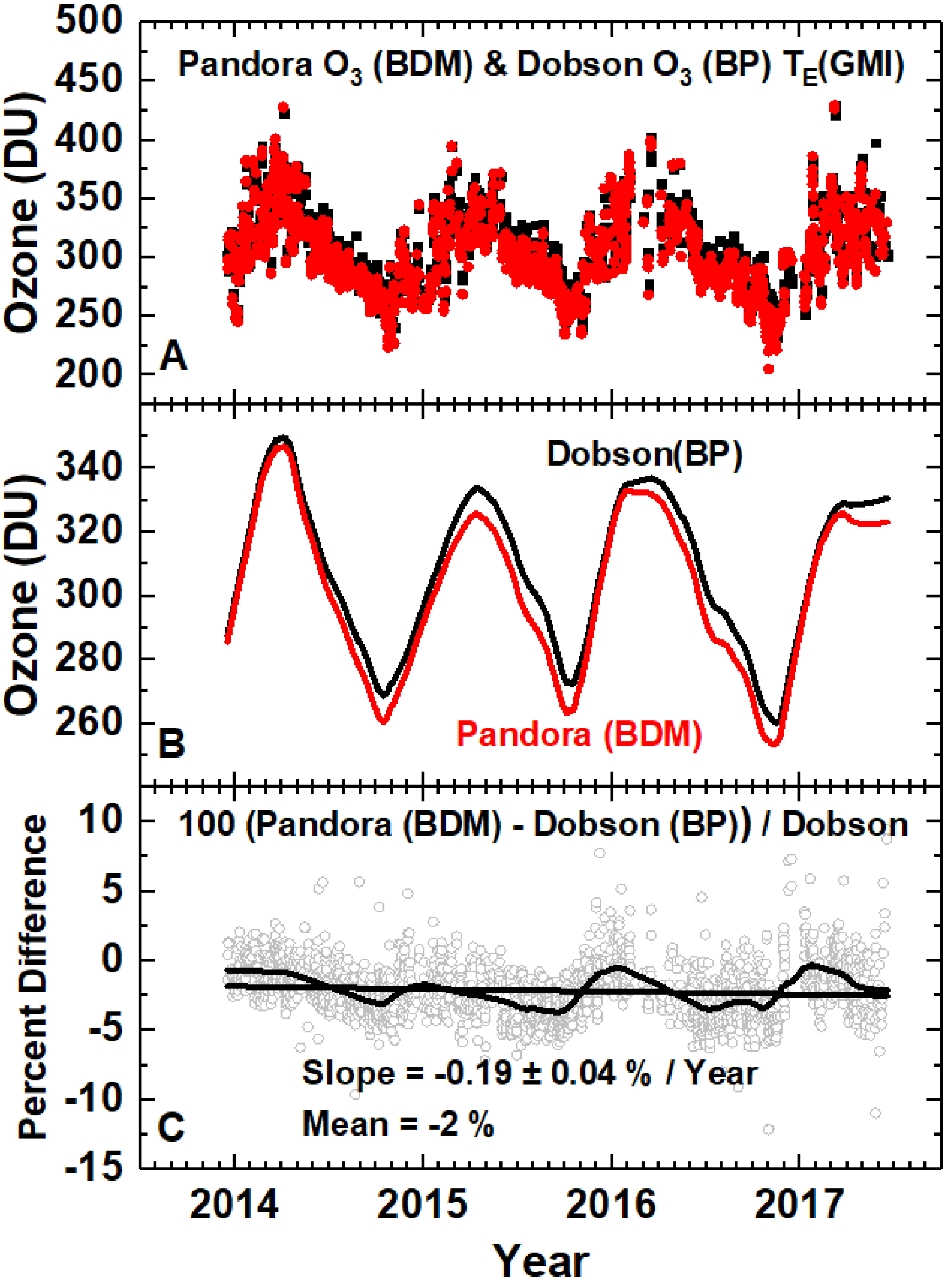

Pandora O_3 (BDM) & Dobson O_3 (BP) T_E(GMI)
Ozone (DU)
500
450
400
350
300
250
200
A
Dobson(BP)
Pandora (BDM)
340
320
300
280
260
B
100 (Pandora (BDM) - Dobson (BP)) / Dobson
Percent Difference
10
5
0
-5
-10
-15
Slope = -0.19 ± 0.04 % / Year
Mean = -2 %
C
2014
2015
2016
2017
Year

F2

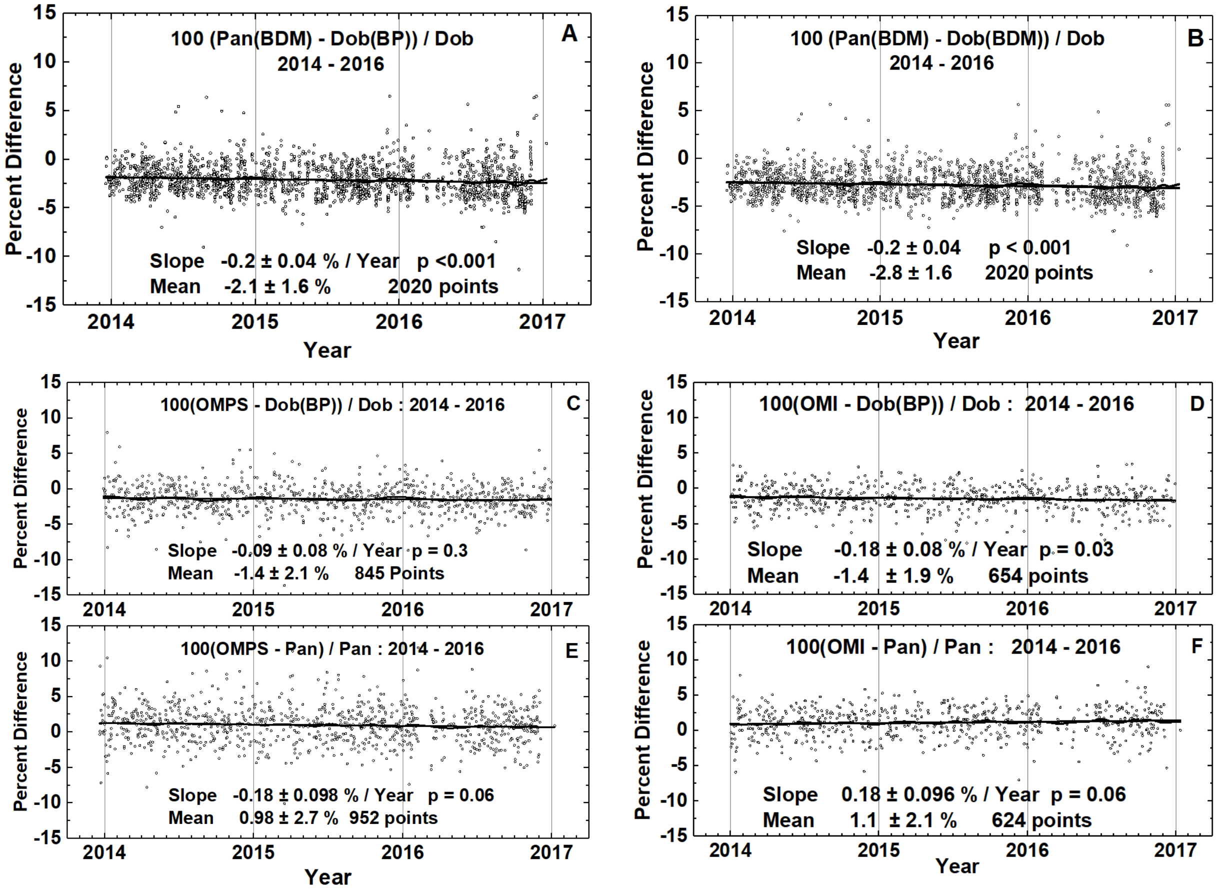

100 (Pan(BDM) - Dob(BP)) / Dob
2014 - 2016
A
Slope -0.2 ± 0.04 % / Year p <0.001
Mean -2.1 ± 1.6 % 2020 points
100 (Pan(BDM) - Dob(BDM)) / Dob
2014 - 2016
B
Slope -0.2 ± 0.04 p < 0.001
Mean -2.8 ± 1.6 2020 points
100(OMPS - Dob(BP)) / Dob : 2014 - 2016
C
Slope -0.09 ± 0.08 % / Year p = 0.3
Mean -1.4 ± 2.1 % 845 Points
100(OMI - Dob(BP)) / Dob : 2014 - 2016
D
Slope -0.18 ± 0.08 % / Year p = 0.03
Mean -1.4 ± 1.9 % 654 points
100(OMPS - Pan) / Pan : 2014 - 2016
E
Slope -0.18 ± 0.098 % / Year p = 0.06
Mean 0.98 ± 2.7 % 952 points
100(OMI - Pan) / Pan : 2014 - 2016
F
Slope 0.18 ± 0.096 % / Year p = 0.06
Mean 1.1 ± 2.1 % 624 points
Percent Difference
Year
15
10
5
0
-5
-10
-15
2014
2015
2016
2017

F3

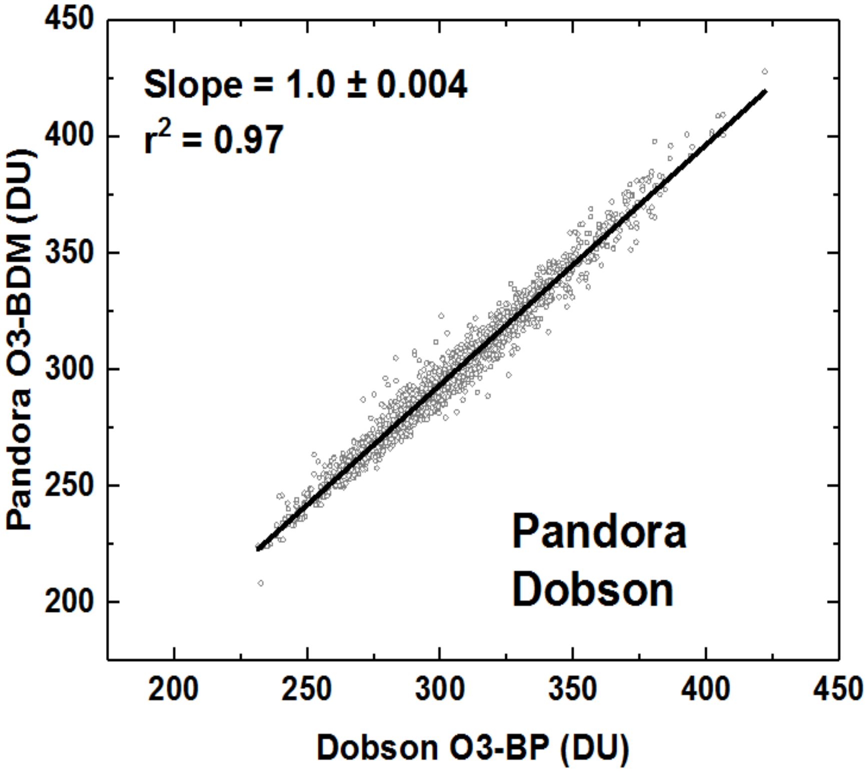
Slope = 1.0 ± 0.004
r^2 = 0.97
Pandora
Dobson
Pandora O3-BDM (DU)
Dobson O3-BP (DU)
200
250
300
350
400
450
200
250
300
350
400
450

F4

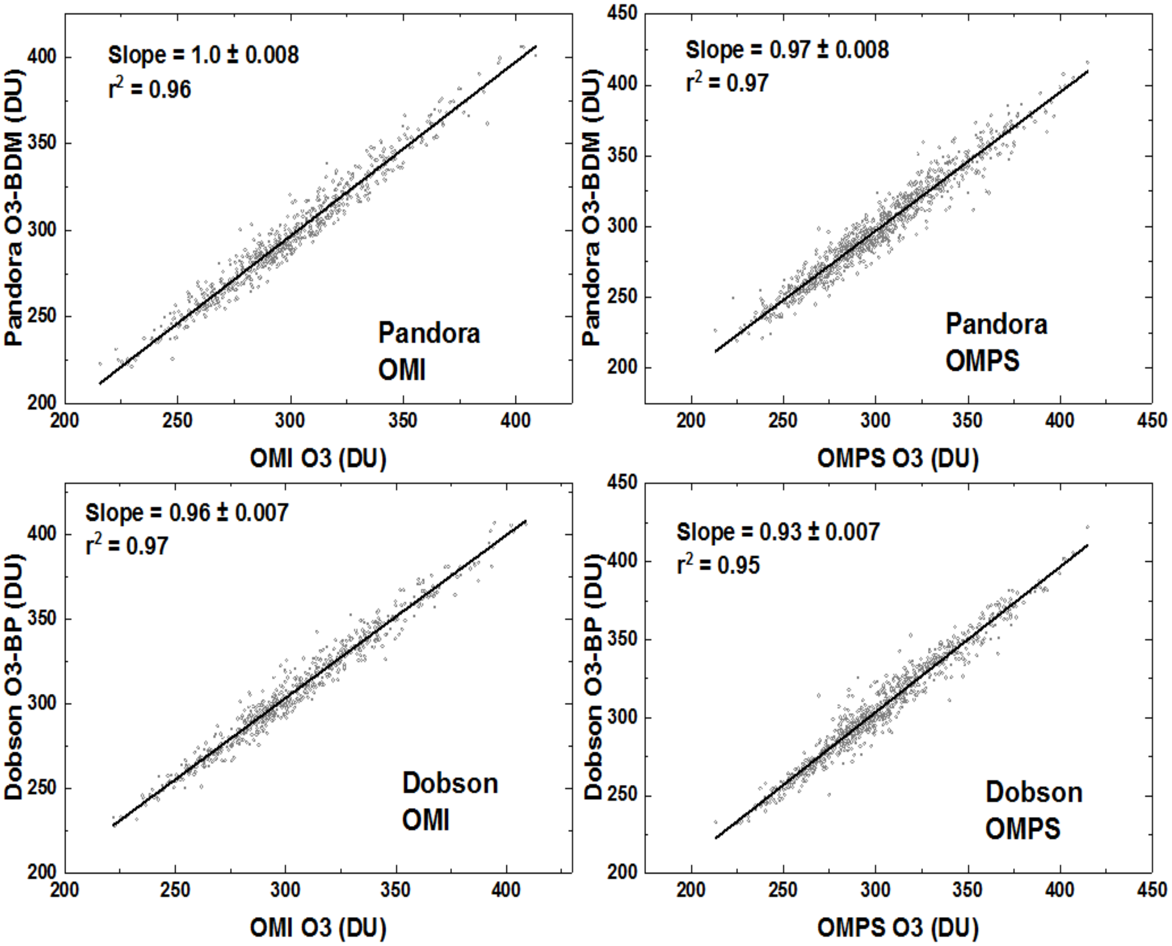
Slope = 1.0 ± 0.008
r² = 0.96
Pandora
OMI
Pandora O3-BDM (DU)
OMI O3 (DU)
200
250
300
350
400
Slope = 0.97 ± 0.008
r² = 0.97
Pandora
OMPS
Pandora O3-BDM (DU)
OMPS O3 (DU)
200
250
300
350
400
450
Slope = 0.96 ± 0.007
r² = 0.97
Dobson
OMI
Dobson O3-BP (DU)
OMI O3 (DU)
Slope = 0.93 ± 0.007
r² = 0.95
Dobson
OMPS
Dobson O3-BP (DU)
OMPS O3 (DU)

F5